

Personalizing the Treatment of Pediatric Medulloblastoma: Polo-like Kinase 1 as a Molecular Target in High-Risk Children

Joanna Triscott¹, Cathy Lee¹, Colleen Foster², Branavan Manoranjan⁵, Mary Rose Pambid¹, Rachel Berns¹, Abbas Fotovati¹, Chitra Venugopal⁵, Katrina O'Halloran¹, Aru Narendran⁷, Cynthia Hawkins⁶, Vijay Ramaswamy⁶, Eric Bouffet⁶, Michael D. Taylor⁶, Ash Singhal³, Juliette Hukin¹, Rod Rassekh¹, Stephen Yip⁴, Paul Northcott⁸, Sheila K. Singh⁵, Christopher Dunham², and Sandra E. Dunn¹

Abstract

Medulloblastoma is the most common malignant brain tumor in children. This disease is heterogeneous and is composed of four subtypes of medulloblastoma [WNT, Sonic Hedgehog (SHH), Group 3, and Group 4]. An immediate goal is to identify novel molecular targets for the most aggressive forms of medulloblastoma. Polo-like kinase 1 (PLK1) is an oncogenic kinase that controls cell cycle and proliferation, making it a strong candidate for medulloblastoma treatment. In this study, pediatric medulloblastomas were subtyped in two patient cohorts (discovery cohort, $n = 63$ patients; validation cohort, $n = 57$ patients) using NanoString nCounter analysis and *PLK1* mRNA was assessed. We determined that the SHH and Group 3 subtypes were independently associated with poor outcomes in children as was PLK1 using Cox regression analyses. Furthermore, we screened a library of 129 compounds in clinical trials using a model of pediatric medulloblastoma and determined that PLK1 inhibitors were the most promising class of agents against the growth of medulloblastoma. In patient-derived primary medulloblastoma isolates, the PLK1 small-molecule inhibitor BI2536 suppressed the self-renewal of cells with high PLK1 but not low PLK1 expression. PLK1 inhibition prevented medulloblastoma cell proliferation, self-renewal, cell-cycle progression, and induced apoptosis. In contrast, the growth of normal neural stem cells was unaffected by BI2536. Finally, BI2536 extended survival in medulloblastoma-bearing mice with efficacy comparable with Headstart, a standard-of-care chemotherapy regimen. We conclude that patients with medulloblastoma expressing high levels of *PLK1* are at elevated risk. These preclinical studies pave the way for improving the treatment of medulloblastoma through PLK1 inhibition. *Cancer Res*; 73(22); 6734–44. ©2013 AACR.

Introduction

Medulloblastoma is the most common malignant pediatric brain tumor. The current treatment for medulloblastoma

entails maximal safe resection, whole brain and spinal cord radiation for children older than 3, and aggressive chemotherapy. The advances in medical treatments have improved patient survival from 5% in the 1960s (1) to more than 70% for the standard-risk disease (2, 3). Yet, the 5-year survival rate for the high-risk disease is still dismal (16%–70%; ref. 3), and almost all survivors will inevitably suffer from adverse, lifelong consequences from treatment. These undesirable effects are attributable to the detrimental impacts that surgical procedures, radiotherapy, and chemotherapy have on the developing brain (4). Therefore, there is an imperative need to identify novel therapeutics that could improve the cure rate while avoiding harmful side effects.

Medulloblastoma can be divided into four different molecular subtypes, namely, WNT, Sonic Hedgehog (SHH), Group 3, and Group 4. These subtypes were originally described on the basis of differences in gene expression using cDNA microarrays (5), which were subsequently substantiated by immunohistochemistry (IHC; refs. 5, 6). Microarrays are problematic because they require fresh snap-frozen tissues, whereas IHC is hindered by the subjectivity of scoring and differential staining across laboratories. Recently, mRNA-based assays have been developed using the Nanostring nCounter system

Authors' Affiliations: ¹Department of Pediatrics; ²Division of Anatomic Pathology, Department of Pathology and Laboratory Medicine; ³Division of Pediatric Neurosurgery, Department of Surgery, BC Children's Hospital, University of British Columbia; ⁴Department of Pathology and Laboratory Medicine, Centre for Applied Genomics, British Columbia Cancer Agency, Vancouver, British Columbia; ⁵Division of Neurosurgery, Department of Surgery, Faculty of Health Sciences, McMaster Stem Cell and Cancer Research Institute, McMaster University, Hamilton; ⁶The Arthur and Sonia Labatt Brain Tumor Research Centre, Hospital for Sick Children, Toronto, Ontario; ⁷Pediatric Oncology Experimental Therapeutics Investigators Consortium (POETIC) Laboratory for Pre-Clinical and Drug Discovery Studies, Division of Pediatric Oncology, Alberta Children's Hospital, Calgary, Alberta, Canada; and ⁸Division of Pediatric Neuro-Oncology, German Cancer Research Center (DKFZ), Heidelberg, Germany

Note: Supplementary data for this article are available at Cancer Research Online (<http://cancerres.aacrjournals.org/>).

Corresponding Authors: Sandra E. Dunn, Department of Pediatrics, University of British Columbia, 950 West 28th Avenue, Vancouver, BC, Canada V5Z 4H4. Phone: 604-875-2000, ext. 6015; Fax: 604-875-3120; E-mail: sedunn@mail.ubc.ca; and Christopher Dunham, E-mail: cdunham@cw.bc.ca.

doi: 10.1158/0008-5472.CAN-12-4331

©2013 American Association for Cancer Research.

to avoid some of the problems associated with prior methods of classification (5). Advantages of NanoString are as follows: (i) multiple genes are used to distinguish medulloblastoma subtypes, (ii) it is highly quantitative, and (iii) it does not require an amplification step, allowing for low-abundance genes to be detected from formalin-fixed paraffin-embedded (FFPE) tissues.

The medulloblastoma subtypes differ not only in genetic signatures but also in response to clinical therapy (7). In studies of medulloblastoma in which adult and pediatric patients were evaluated collectively, the WNT molecular subtype was associated with the best prognosis, whereas the Group 3 tumors fair the poorest. The SHH and Group 4 tumors correlate with intermediate outcomes in studies that captured adult and pediatric patients (5, 8). However, it is not known whether the risk associated with each subtype holds true when the cohort is solely composed of pediatric patients.

Extensive insights into the biology of the SHH pathway have spearheaded significant progress into the development of related targeted therapies, notably to Smoothed (SMO) for which there are several open clinical trials (9). There are already reports of acquired resistance due to point mutations in *SMO* (10), amplification in *GLI2* (11), and signaling through the PI3K pathway (12). It is therefore possible that other signal transduction pathways may provide alternative approaches to the management of medulloblastoma. The identification of targeted therapies for Group 3 and Group 4 tumors also remains a challenge. We provide clinical and preclinical evidence suggesting that Polo-like kinase 1 (PLK1) is a provocative molecular target for pediatric medulloblastoma that transcends molecular subtypes.

Materials and Methods

Medulloblastoma patient cohorts

Primary medulloblastoma samples were obtained from BC Children's Hospital (Vancouver, BC, Canada; discovery) and The Hospital for Sick Children (Toronto, ON; validation). In the discovery cohort, we obtained 75 tumor blocks from patients diagnosed with medulloblastoma between 1986 and 2012. The samples included both primary and relapse specimens; however, only primary samples were assessed in this study. Medical charts were reviewed and pertinent clinicopathologic data were recorded (R. Rassekh, K. O'Halloran, and C. Foster). Patient ages ranged from 3 months to 16.8 years; a review of this cohort is shown in Supplementary Table S1. Twelve of 75 patients were excluded from survival analysis. Three patient samples were retrospectively found to be misdiagnoses, and 9 other patients received a treatment regimen conflicting with the standard-of-care. Dr. Michael D. Taylor from The Hospital for SickKids, University of Toronto, generously provided the validation cohort of 61 patients with medulloblastoma (Supplementary Table S2). Four of 61 patients were excluded from survival analysis for the purpose of homogeneity of treatment. All tumors were subtyped and the data were analyzed according to Northcott and colleagues (13).

NanoString nCounter gene expression profiling

RNA was extracted from three 20- μ m scrolls of FFPE tissue using the Qiagen RNeasy FFPE Kit. Exactly 250 ng of RNA was run for each patient sample and RNA quality was assessed using Nanodrop spectrometry. A 2100 Bioanalyzer (Agilent Technologies) was used to spot-check RNA quality in random samples. Medulloblastoma cell lines were grown as tumorspheres, and subsequent mRNA analysis was performed in a similar manner to the FFPE tissues. Analysis using the nCounter Gene Expression system was conducted at the Centre for Translational and Applied Genomics (BC Cancer Agency, Vancouver, BC, Canada). A custom codeset synthesized by NanoString Technologies was designed, which included 22 medulloblastoma-specific subtyping gene probes (13) plus other genes of interest that specifically included *PLK1* (NM_005030.3). The recommendations outlined by NanoString Technologies were all followed for sample preparation, hybridization, detection, scanning, and data normalization.

Gene expression and subtype assignment analysis

NanoString gene expression data were analyzed as previously described (8, 13–15). Cell lines (grown as neurospheres) and xenograft tumor tissues were assigned subgroup classification using the 72-patient cohort as a training set. Cutoff points for *PLK1* expression were assigned on the basis of z score deviation from the mean expression of the cohort. *PLK1* transcript counts fewer than 400 (per 250 ng patient RNA) were considered low in expression. Heatmaps were generated using unsupervised hierarchical clustering with average linkage using Cluster version 3.0 and Treeview version 1.60.

Immunofluorescence

Immunofluorescence staining was performed on Daoy cells according to the procedure we previously described (16). Primary antibodies include α -tubulin (ab18251; Abcam), Pericentrin (ab28144; Abcam), anti-P-H2AX^{S139} (ab26350; Abcam), and PARP (Cell Signaling Technology). Images were taken using an Olympus FV10i confocal microscope on $\times 60$ magnification.

Drug library screen

The small-molecule-targeted therapeutic agents were synthesized, purity checked, and purchased from ChemieTek. The Daoy cell line was seeded (3,000 cells/well) overnight and then treated with 1 and 10 μ mol/L for 72 hours. Cells were fixed in 2% paraformaldehyde and stained with Hoechst 33342 (1 μ g/mL; Sigma-Aldrich). Analysis was done with the ArrayScan high-content screening system (Thermo Fisher Scientific).

Cell culture and tumorsphere growth

Daoy cells were obtained from the American Type Culture Collection. Primary brain tumor cells were isolated from BTX001 (SHH), BT006 (SHH), BT007 (SHH), BT008 (PNET), BT014 (Group 4), BT274 (SHH), and BT025 (Group 4) and were grown as neurospheres as previously described (17) using Neurocult media (StemCell Technologies; ref. 18). All primary cells were obtained through informed consent in accordance with the respective research ethics board guidelines at British Columbia Children's Hospital and The Hospital for Sick

Children. A single-cell suspension of Daoy and patient-derived primary medulloblastoma cells (BTX001, BT274, BT014, and BT025) were plated in tumorsphere assays as previously described (18). Tumorspheres, plated in triplicate more than 50 μm , were quantified and photomicrographs were taken after 6 days of culture.

Transfection and western blotting

siRNA transfections were performed using Lipofectamine RNAiMAX (Invitrogen) as previously described (19). Immunoblotting was conducted using anti-PLK1 (Sigma-Aldrich), anti-P-CDC25C^{Ser198}, anti-P-TCTP^{Ser46}, and anti-pan-actin (Cell Signaling Technology). Band densitometry was measured using ImageJ, v1.46r and normalized to actin.

Cell-cycle analysis

Cell-cycle analysis was done following 24-hour siRNA or BI2536 treatment using flow cytometry as described by Lee and colleagues (2012) (18). Histone H3 phosphorylation was tested as previously described using P-histone H3^{Ser10} (Cell Signaling Technology; ref. 20).

Annexin V staining and quantification of cell growth by Hoechst staining

Daoy cells were treated with 2.5 nmol/L BI2536 for 48 hours and stained with Annexin V (Promega) as previously described (21). To evaluate the effect of PLK1 inhibition on cell growth, Daoy or human neural stem cells (hNSC; H9, hESC-derived, GIBCO) were also plated (3,000 cell/well) in 96-well plates following previously outlined methods (19, 21).

In vivo evaluation of BI2536 compared with chemotherapy

Xenografts from Daoy cell lines were injected into the right frontal lobe of NOD-CB17-SCID mouse brains according to Research Ethics Board–approved protocols ($n = 18$). Mice were injected with biologic replicates consisting of 10^6 single-cell suspensions and randomly divided into three treatment groups ($n = 6$) following engraftment of orthotopic tumors: control (0.1N HCl), chemotherapy (vincristine, cisplatin, and cyclophosphamide), and treatment (BI2536). Intraperitoneal injections were performed for delivery of all study-group agents. The control group consisted of one weekly injection of 0.1N HCl for 4 weeks. The chemotherapy group modeled a Headstart protocol that consisted of one weekly injection of vincristine (1.05 $\mu\text{g}/\text{kg}$) and cisplatin (2.5 mg/kg) on day 1 followed by cyclophosphamide (0.0352 mg/kg) on day 2 for 3 weeks. The treatment group consisted of one weekly injection of BI2536 (62.5 mg/kg , diluted in 0.1N HCl) for 4 weeks. The mice were observed until they displayed obvious signs of neurologic deficits and appeared unwell. Tumors were removed at the end of the study, FFPE, and stained with hematoxylin and eosin. The histopathologic diagnosis of the tumors was evaluated by a pediatric neuropathologist (C. Dunham).

Statistical analysis

All quantitative data presented were analyzed as mean value \pm SE. Principal component analysis (PCA) was conducted for

2D modeling of dimensionality reduction of the 22 subtyping genes (8, 13) using Partek Genomics Suite (Partek). For the tissue microarray, clinical survival analysis, and animal studies, log-rank analysis was performed on the Kaplan–Meier curve to determine statistical significance of the results. Multivariate survival analysis was conducted using Cox regression proportional hazards and a 95% confidence interval (CI). All survival analyses and the Spearman's rank correlation test were done using SPSS version 20.0 statistical software (IBM). The number of samples used and the respective P-values are listed in the figure legends. The level of significance for the *in vitro* cell growth/death data was determined by a Student two-tailed *t* test and the difference in *PLK1* expression between subtypes was assessed using one-way ANOVA (*, $P < 0.05$; **, $P < 0.01$).

Results

Medulloblastoma tumor samples were assigned molecular subtype classification using gene expression data and PAM class predication statistical software (Supplementary Tables S3 and S4). On the basis of these subtypes, patients with SHH and Group 3 tumors had high probabilities of relapse (Fig. 1A) and death (Fig. 1B). Children with WNT or Group 4 tumors relapsed less frequently and lived longer (Fig. 1A and B); this was also seen in a separate validation cohort (Supplementary Fig. S1A and S1B). In the discovery cohort, a heatmap of the patient gene expression illustrates the subtype distribution and includes the patient tumors from which tissue specimens were collected for primary cell culture (Fig. 1C). These data prompted us to address whether there may be drugs in clinical trials for adult cancers that would be beneficial for combating SHH type tumors in children; therefore, we subtyped four medulloblastoma cell lines (ONS76, UW228, UW426, and Daoy). Using the 22 established medulloblastoma subtyping genes from Northcott and colleagues (13), each of the cell lines clustered most similarly to the SHH patient subgroup, following both hierarchical clustering (Fig. 1C and Supplementary Fig. S1C) and PCA analysis (Fig. 1D). This classification was verified using PAM (PAM-SHH = $1.0^E + 00$; Supplementary Table S3) and was confirmed again using analysis in which the validation cohort acted as the data training set (data not shown; refs. 13, 14). Subsequently, we conducted a drug library screen in Daoy cells against 129 drugs, most of which are in clinical trials. To be carried forward, compounds had to meet specific criteria: (i) $\geq 70\%$ growth inhibition, (ii) activity at 1 $\mu\text{mol}/\text{L}$ and more so with 10 $\mu\text{mol}/\text{L}$, (iii) potential to cross the blood–brain barrier, (iv) currently in clinical trials, and (iv) novelty. Initially, 11 of 129 compounds partially fulfilled these criteria. Some compounds had shown toxicity in clinical trials or were previously studied. Therefore, we chose to pursue PLK1 because of its relative novelty as a target and the 90% growth inhibition efficacy demonstrated by the PLK1 inhibitor group: BI6727, BI2536, and GSK461364 (Fig. 2A).

In patients, *PLK1* levels were compared with normal cerebellum. *PLK1* mRNA was higher in the vast majority of medulloblastoma than in normal cerebellum using the nCounter system ($P < 0.001$; Fig. 2B and Supplementary Fig. S2A). There was no significant difference in *PLK1* expression among the four medulloblastoma subtypes (Supplementary Fig. S2B). The

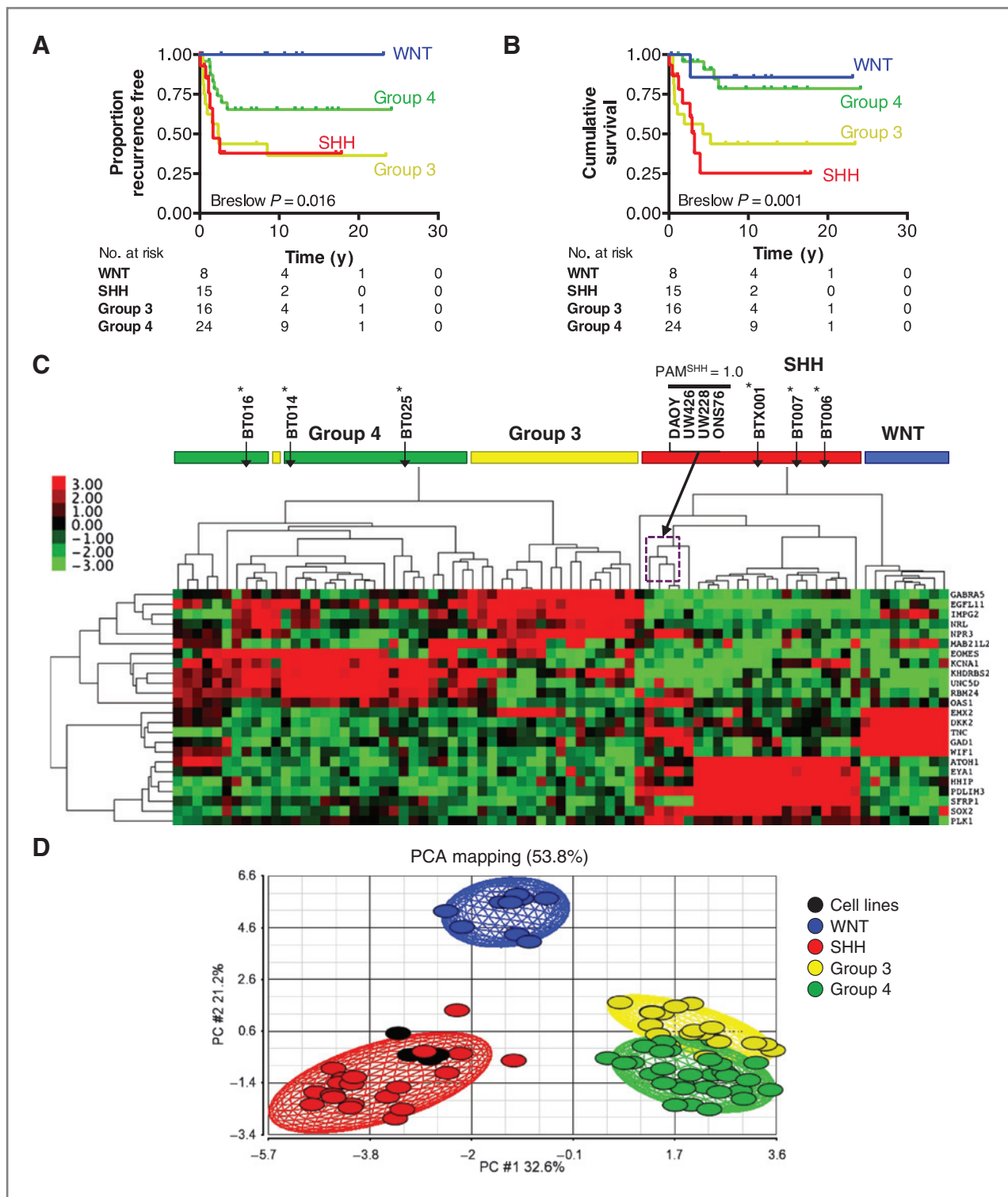


Figure 1. Molecular characteristics of medulloblastoma dictate outcome and offer potential drug targets. A and B, patients with the SHH subtype of medulloblastoma had the highest rates of relapse and the worst chance of overall survival, respectively. C, the patients as well as four medulloblastoma cell lines were subtyped into the different categories based on gene expression and are represented using a heatmap (red, high expression; green, low expression). Cell lines (ONS76, UW228, UW426, and Daoy) were all statistically classified as SHH ($PAM = 1.0^E + 00$). *, patients from which the indicated primary cell cultures were established. D, PCA uses dimensionality reduction of the 22 minimal marker genes (13) to show the association of cultured cells with the medulloblastoma subgroups. The circles represent individual patients (WNT, blue; SHH, red; Group 3, yellow; Group 4, green). The black circles represent cell lines grown as neurospheres (Daoy, ONS76, UW228, UW426). Black circles, cell lines grown as neurospheres (Daoy, ONS76, UW228, and UW426).

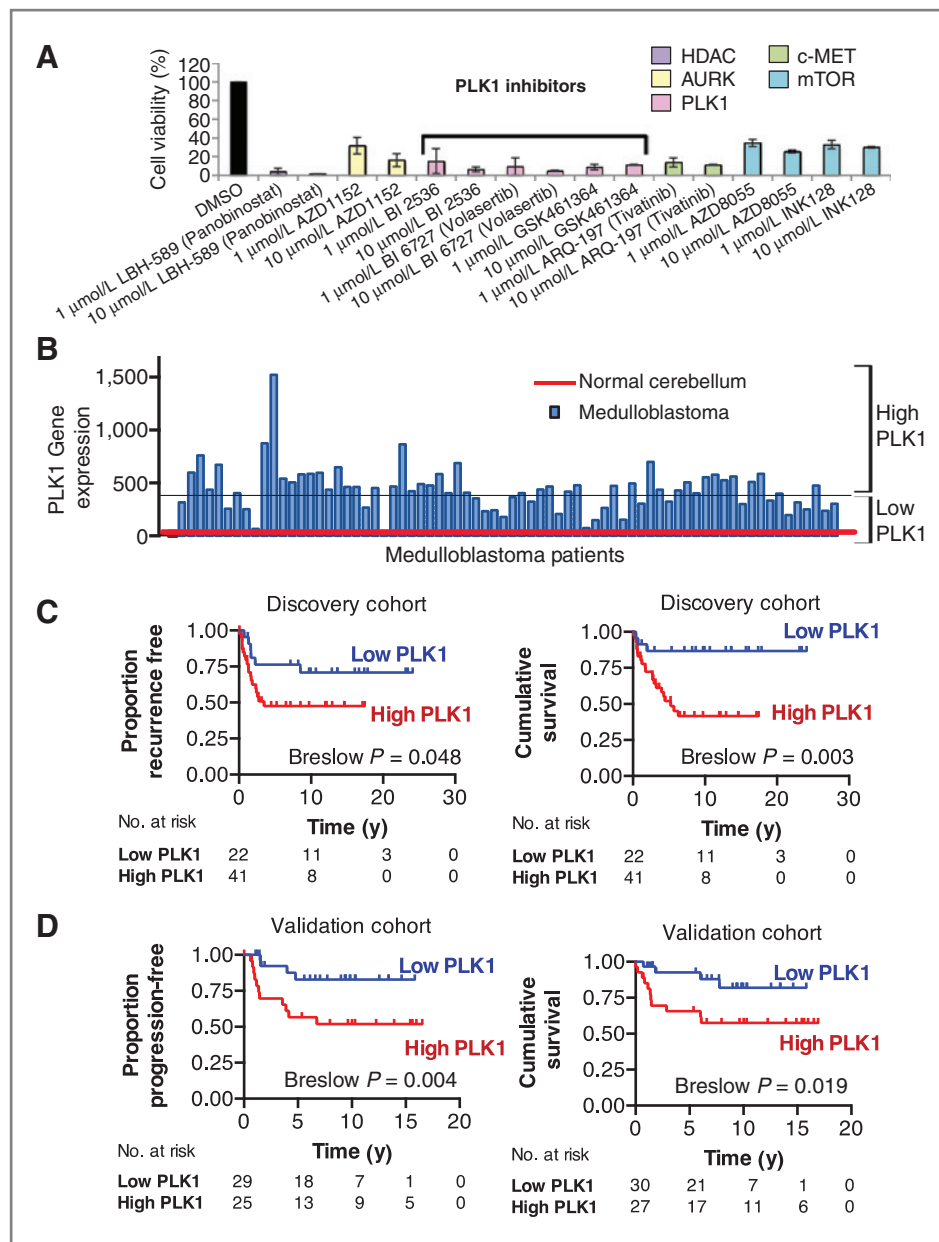


Figure 2. *PLK1* expression correlates with poor patient survival. A, a library of 129 small molecule inhibitors was screened against Daoy cells in a 72-hour growth assay. B, NanoString nCounter analysis of 72 patient samples (blue bars) shows that *PLK1* mRNA is overexpressed in medulloblastoma compared with normal cerebellum (red line) and indicates a cutoff between high and low expressors. C, high *PLK1* mRNA expression predicts probability of patient relapse ($n = 63$, $P = 0.048$) and poor overall survival ($n = 63$, $P = 0.003$), and is validated in a second independent cohort (D) from Toronto, ON (progression-free survival, $n = 54$, $P = 0.04$; overall survival, $n = 57$, $P = 0.019$).

mRNA expression of *PLK1* was associated with higher rates of relapse and poor survival as shown in a Kaplan–Meier univariate analysis (Fig. 2C). In the validation cohort, *PLK1* mRNA levels were also predictive of outcome (Fig. 2D). There was no significant difference in the overall survival outcomes or *PLK1* expression between the study cohorts (Supplementary Fig. S2C).

Multivariate survival analyses of the discovery and validation cohorts are shown in Table 1 and Supplementary Table S5, respectively. The variables identified as independent factors affecting patient survival include presence of metastasis (HR, 3.920; 95% CI, 1.083–14.198), having an SHH medulloblastoma (HR, 9.982; 95% CI, 1.587–62.765), a Group 3 medulloblastoma (HR, 8.874; 95% CI, 1.778–44.283), and expression of *PLK1* (HR,

7.286; 95% CI, 1.469–36.142). Likewise, having SHH medulloblastoma, Group 3 medulloblastoma, and expression of *PLK1* were also significant in the validation cohort (Supplementary Table S5). Younger patients often do poorly as protocols for children younger than age 3 avoid radiotherapy (22). This brings us to question whether cases not receiving radiotherapy had even worse outcomes (22). Age and radiotherapy treatment were significantly associated with univariate survival analysis, but were not independent prognostic markers in the multivariate analysis. In addition, clinical characteristics such as sex, extent of resection, and chemotherapy were not significant variables associated with survival in the log-rank test (Table 1). Neither age nor radiotherapy was significant in the validation cohort (Supplementary Table S5).

Table 1. Univariate and multivariate analyses of clinical, pathologic, and biologic endpoints of the discovery cohort

Variable	Number	Log-rank test (P)	n = 56	HR (95% CI)	Cox regression analysis (P)
Age					
<3 years	14	0.108 (NS)	11	0.886 (0.231–3.390)	0.859 (NS)
≥3 years	49		45		
Sex					
Male	38	0.324 (NS)	34	0.862 (0.267–2.786)	0.804 (NS)
Female	25		22		
Metastasis					
Present	27	0.026	25	3.920 (1.083–14.198)	0.037
Not present	30		31		
Extent of resection					
Gross total resection	47	0.663 (NS)	44	1.187 (0.285–4.946)	0.814 (NS)
Subtotal resection or less	14		12		
Radiotherapy					
Yes	48	0.102 (NS)	42	1.688 (0.420–6.785)	0.461 (NS)
No	15		14		
Chemotherapy					
Yes	57	0.938 (NS)	52	3.708 (0.317–43.421)	0.296 (NS)
No	6		4		
SHH subtype					
SHH	15	0.007	14	9.982 (1.587–62.765)	0.014
Non-SHH	48		42		
Group 3 subtype					
Group 3	16	0.046	13	8.874 (1.778–44.283)	0.008
Non-Group 3	47		43		
PLK1 transcript					
High	41	0.001	36	7.286 (1.469–36.142)	0.015
Low	22		20		

Abbreviation: NS, not statistically significant.

Primary patient-derived medulloblastoma cells were obtained from surgical specimens and grown as tumorspheres (BTX001, BT014, BT016, and BT025). RNA was extracted from cultured tumorspheres and compared with matched FFPE sections from the original tumor whereby their gene expression was characterized using nanoString. Cultured primary cells retained subtype and *PLK1* expression patterns of the original tumors. This is exemplified with BTX001, BT016 (Fig. 3A), and BT025 (Supplementary Fig. S3A). Interestingly, *PLK1* mRNA was higher in BTX001 than in normal cerebellum (CB) or hNSC by qRT-PCR (Fig. 3B) and BI2536 BTX001 hindered self-renewal upon serial passaging (Fig. 3C). In contrast, BT014 and BT025 cells were derived from Group 4 tumors that expressed low levels of *PLK1* (Fig. 3B and Supplementary Fig. S3B) and they were not responsive to BI2536 (Fig. 3C and Supplementary Fig. S3C). Importantly, the growth effects of hNSCs were negligible when screened with BI2536 as an *in vitro* evaluation for the safety (Fig. 3D). Expression of *PLK1* mRNA in additional freshly isolated primary specimens (BTX001, BT006, BT007, BT274, and BT008) was higher than normal human astrocytes, which are another predominant brain cell type. Daoy *PLK1*

expression was also comparable with the primary medulloblastoma freshly isolated from patients (Supplementary Fig. S3D).

PLK1 inhibition with siRNA suppressed the Daoy growth by approximately 90% in 72 hours (Fig. 4A and B). Deactivation of PLK1 activity was confirmed by downregulation of phosphorylation of its direct substrate, translationally controlled tumor protein (TCTP), by approximately 80% (Fig. 4A; refs. 23, 24). *PLK1* levels expressed in Daoy cells were similar to the levels found in poor prognosis of patients with medulloblastoma (Supplementary Fig. S4A). Likewise, PLK1 protein and mRNA expression was detected in two additional medulloblastoma cell lines ONS76 and UW426 (Supplementary Fig. S4A and S4B), which were equally sensitive to PLK1 inhibition (Supplementary Fig. S4C). As expected, BI2536 suppressed phosphorylation of the known PLK1 substrates TCTP and CDC25C and reduced cell growth with an IC₅₀ of 5 nmol/L at 72 hours (Fig. 4B). BI2536 treatment at 24 hours halted the cell cycle and caused G₂-M arrest with observable compromised cell cycle and division as shown by immunofluorescence staining (Fig. 4C and Supplementary Fig. S4D). PLK1 inhibition in Daoy cells resulted in irregular centrosome duplication and separation with many cells appearing

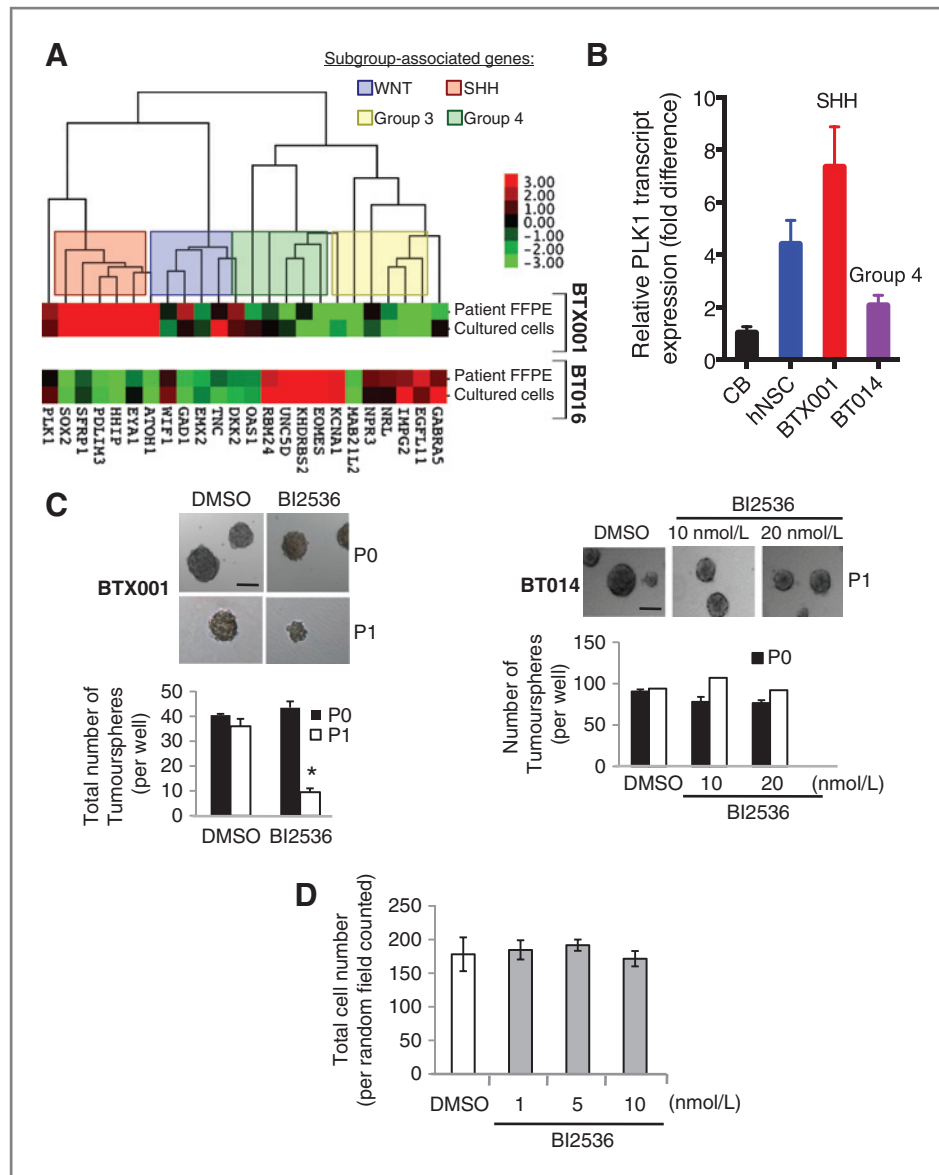


Figure 3. The response of primary medulloblastoma cells to BI2536 is correlated with the expression of PLK1 in the tumors. **A**, primary cultured medulloblastoma cells retain gene expression characteristics of the tumor of origin as demonstrated using NanoString analysis of mRNA extracted from primary cultured cells and FFPE tissue from matched origin patient tumors. BTX001 exemplifies a high *PLK1* SHH tumor and BT016 as a low *PLK1* Group 4 tumor. **B**, *PLK1* mRNA from the cerebellum (CB) tissue, hNSCs, patient-derived SHH medulloblastoma sample BTX001, and patient-derived Group 4 medulloblastoma BT014. **C**, BI2536 (10 nmol/L) inhibited the self-renewal of BTX001 over 6 days (*, $P < 0.05$; scale bar, 140 μm). BT014 were not responsive to 10 nmol/L BI2536 (6-day treatment; scale bar, 140 μm). **D**, hNSCs were treated with 1, 5, and 10 nmol/L of BI2536 for 72 hours, stained with Hoechst dye. BI2536, even at the highest dose tested (10 nmol/L), had a negligible impact on their growth.

polynucleated relative to control treatments (Fig. 4C and Supplementary Fig. S5). Both siPLK1 and BI2536 treatments induced apoptosis at 48 hours (Fig. 4D) and self-renewal was abolished with 10 nmol/L BI2536 (Supplementary Fig. S6A).

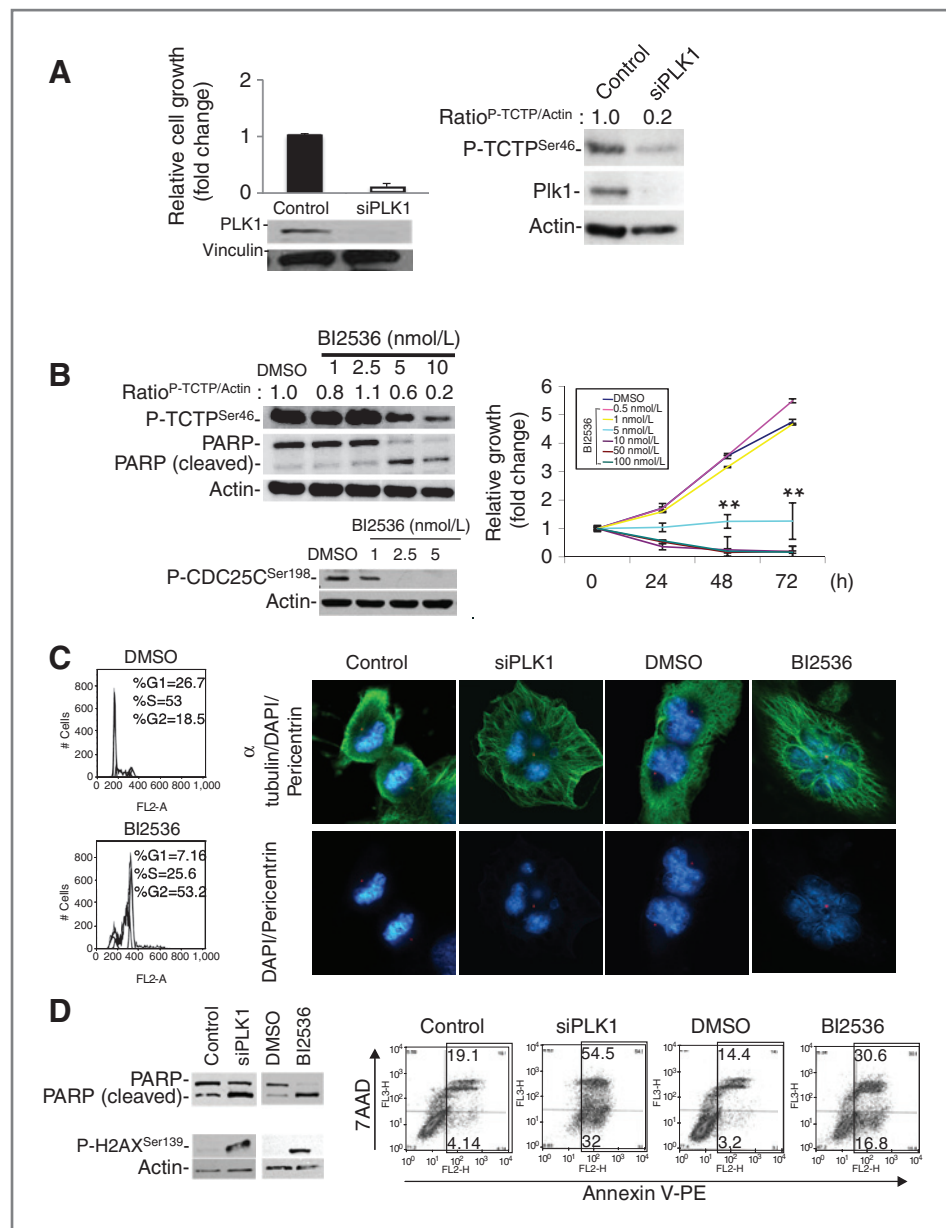
Daoy and two additional medulloblastoma cell lines responded to chemotherapeutic agents (vincristine, cisplatin, and etoposide) that are used for medulloblastoma treatment (Fig. 5A and Supplementary Fig. S6B). Therefore, we used an animal model to compare the *in vivo* efficacy of BI2536 with the conventional chemotherapy using a chemotherapy commonly used in protocol. BI2536 delayed medulloblastoma tumor growth and was comparable with standard-of-care chemotherapy protocols (Fig. 5B). It is important to note that the histomorphology of the Daoy xenografts in our NOD-CB17-SCID mice was also similar to large cell anaplastic (LCA) medulloblastoma (Fig. 5C). This is consistent with a study

reported by Shu and colleagues (25), in which the Daoy cells were injected intracranially into Rag2 severe combined immunodeficient (SCID) mice. LCA histology is often an indication of poor survival in both SHH and Group 3 medulloblastoma (15). The xenografts were then compared with patient-derived medulloblastoma. Notably, their gene signature grouped with patients with SHH subtype (Fig. 5D). The SHH stem cell gene *SOX2* (26) was consistently expressed, as was *GLI2* another transcription factor involved in SHH signaling.

Discussion

Children diagnosed with medulloblastoma were more likely to relapse and die if their tumor was classified in either the Group 3 or SHH subtype. This differs somewhat to previously published studies reporting SHH as an intermediate prognosis (5, 7) and we suspect that this could be due to differences in

Figure 4. PLK1 inhibition suppresses cell growth and induces apoptosis in Daoy cells. A, Daoy cells were treated with 5 nmol/L of PLK1 siRNA for 72 hours, knockdown was confirmed by immunoblotting (bottom), and cell growth was assessed by Hoechst staining (top). Immunoblotting for PLK1 substrate, P-TCTP^{Ser46}, following siPLK1 knockdown. Densitometry quantification normalized to actin housekeeper. B, P-TCTP^{Ser46}, PARP cleavage, and P-CDC25C^{Ser198} in Daoy cells treated with dimethyl sulfoxide (DMSO), 1, 2.5, 5, or 10 nmol/L BI2536 for 48 hours. Daoy cells were treated with 0.5 to 100 nmol/L BI2536 for 24, 48, and 72 hours and then growth was assessed by Hoechst staining. *, $P < 0.05$; **, $P < 0.01$. C, Daoy cells were treated with 5 nmol/L BI2536 for 24 hours and subjected to flow cytometry for analysis of the cell-cycle profile with propidium iodide. PLK1 was inhibited in Daoy cells using siPLK1 or 10 nmol/L BI2536 for 24 hours and then stained for α -tubulin (green), pericentrin (red), and 4',6'-diamidino-2-phenylindole (DAPI) nuclear staining (blue). D, Daoy cells were treated with 5 nmol/L BI2536 for 48 hours. Apoptosis was measured by immunoblotting for PARP cleavage and P-H2AX^{Ser139} or Annexin V-PE/7AAD staining.



the way patients are treated, such as avoiding radiotherapy in younger patients and/or the composition of the patient cohort. In our study, we only included pediatric medulloblastoma, whereas other reports also included adult tumors (5). Furthermore, the SHH subtype in children and adults is associated with different outcomes (15). One of the limitations of our study was the availability of fresh primary tumor tissue from different subtypes. Although only SHH and Group 4 tumors were available to culture during this study's duration, we, nonetheless, hypothesize that our findings have major clinical implications for many medulloblastomas, given that *PLK1* overexpression is prevalent and cuts across molecular subtypes. As we continue culturing incoming patient cells we will extend our study to test our findings in more medulloblastoma.

PLK1 is an oncogenic kinase that confers a growth and survival advantage in cancer cells through its central role in mitosis (27). In multiple cancer models, PLK1 inhibition specifically eliminates the malignant cells while leaving the non-malignant cells unharmed (28–30). Furthermore, PLK1 is highly expressed in cancer cells but not in their normal cell counterparts (31, 32), rendering this kinase a particularly attractive molecular target for cancer therapeutics. Our study tests the PLK1 small-molecule inhibitor, BI2536, which has been evaluated in patients with cancer (33, 34). Various other small molecule inhibitors to PLK1 have been designed and evaluated in phase I/II clinical trials including BI2536, BI6727, Rigosertib, and GSK461364 (35–39). None of these trials have specifically addressed the possibility that PLK1 inhibitors may be beneficial for the treatment of brain tumors. Our group has demonstrated

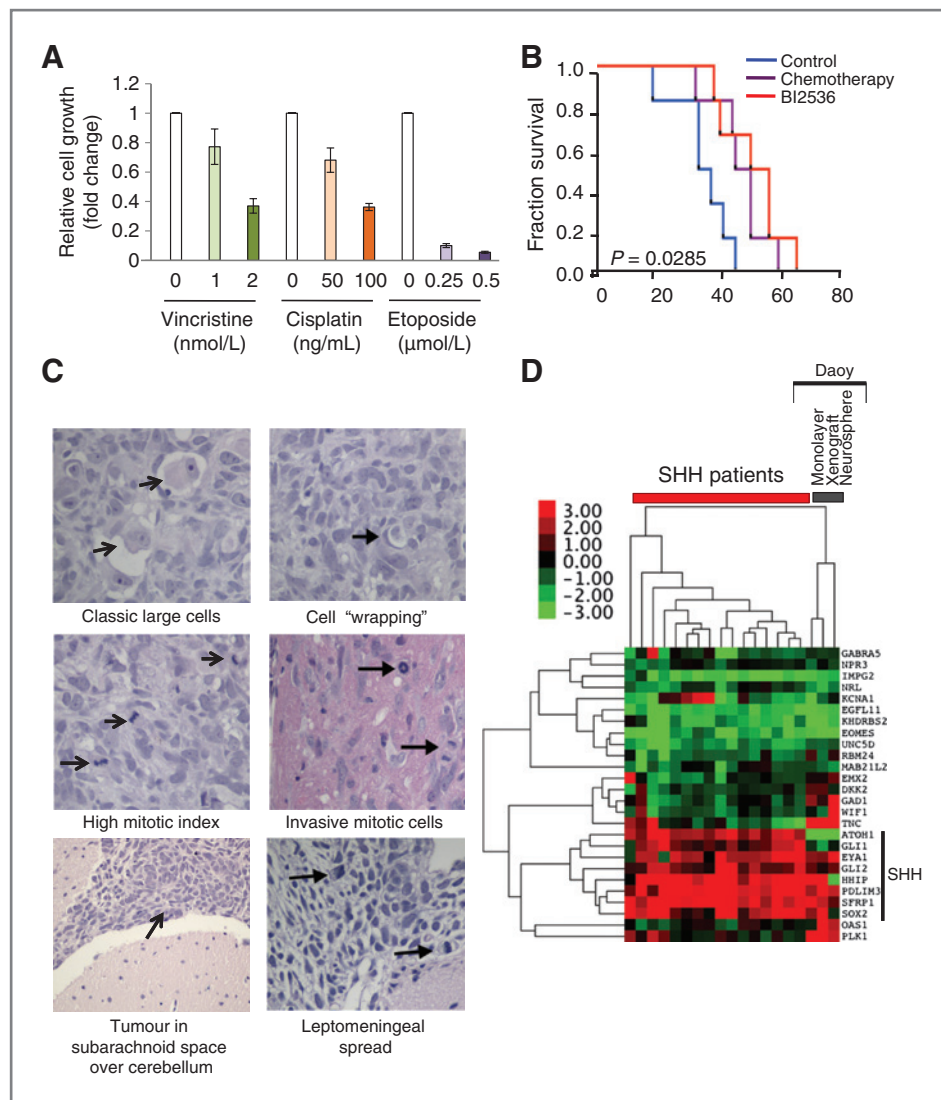


Figure 5. PLK1 inhibition suppresses tumorsphere formation *in vitro* and delayed disease progression *in vivo*. A, Daoy cells were treated with vincristine, cisplatin, or etoposide for 72 hours and stained with Hoechst for quantification. B, Daoy cells were transplanted intracranially into mice and treated with BI2536 ($n = 6$) or chemotherapy ($n = 6$) according to a standard-of-care schedule and compared with control ($n = 6$). BI2536-treated mice lived longer than controls ($P = 0.0142$, log rank) and were comparable with the benefit observed from chemotherapy ($P = 0.0336$). No significant difference in survival was observed between BI2536- and chemotherapy-treated mice ($P = 0.4205$). C, the Daoy xenografts were characterized as having large cellular morphology, cell wrapping, high mitotic activity, and invasion into cerebellum and along the leptomeninges. D, heatmap showing the gene expression of Daoy xenograft tumors that resembled SHH patients from the validation cohort (green, low expression; red, high expression).

that PLK1 inhibitors could be used to target glioblastoma (18, 40) and another group has published data agreeing with our findings in medulloblastoma (41, 42). We illustrate that PLK1 is a promising drug target for medulloblastoma because (i) it is highly expressed in tumors relative to normal brain tissues and (ii) there are small molecule inhibitors that suppress primary medulloblastoma cells and cell lines *in vitro* and *in vivo*.

In conclusion, patients that have tumors expressing very high levels of PLK1 are considered to be at elevated risk for relapse and death. Because there are several PLK1 inhibitors in clinical trials for adult malignancies, we propose that these drugs may also provide benefit for selected patients with medulloblastoma. In the future, it will be desirable to personalize the treatment of medulloblastoma by selecting patients with high PLK1 using accurate, sensitive methods such as that of the NanoString nCounter technology, in which subgroup affiliation of tumors can be assigned rapidly and reproducibly (13). Furthermore, we anticipate that PLK1 inhibitors may have fewer detrimental side effects, as it is not expressed at high

levels in normal brain tissue. Therefore, it could be a great improvement to many of the chemotherapies currently being used that can often cause long-term adverse effects (43). These preclinical studies pave the way for improving the treatment of medulloblastoma through PLK1 inhibition.

Disclosure of Potential Conflicts of Interest

S. Yip has honoraria from Speakers' Bureau from Life Technologies and is a consultant/advisory board member of GLG Consulting. No potential conflicts of interest were disclosed by the other authors.

Authors' Contributions

Conception and design: J. Triscott, C. Lee, A. Singhal, R. Rassekh, C. Dunham, S.E. Dunn

Development of methodology: J. Triscott, C. Lee, A. Fotovati, A. Narendran, M.D. Taylor, R. Rassekh, C. Dunham, S.E. Dunn

Acquisition of data (provided animals, acquired and managed patients, provided facilities, etc.): J. Triscott, C. Lee, C. Foster, B. Manoranjan, M.R. Pambid, R. Berns, A. Fotovati, C. Venugopal, K. O'Halloran, A. Narendran, C. Hawkins, V. Ramaswamy, M.D. Taylor, A. Singhal, R. Rassekh, S.K. Singh, C. Dunham

Analysis and interpretation of data (e.g., statistical analysis, biostatistics, computational analysis): J. Triscott, C. Lee, C. Foster, B. Manoranjan, M.R. Pambid, E. Boufflet, M.D. Taylor, P. Northcott, S.K. Singh, C. Dunham

Writing, review, and/or revision of the manuscript: J. Triscott, C. Lee, C. Foster, B. Manoranjan, M.R. Pambid, R. Berns, K. O'Halloran, A. Narendran, E. Bouffet, M.D. Taylor, A. Singhal, R. Rassekh, S. Yip, P. Northcott, S.K. Singh, C. Dunham, S.E. Dunn

Administrative, technical, or material support (i.e., reporting or organizing data, constructing databases): A. Narendran, A. Singhal, S. Yip, C. Dunham, S.E. Dunn

Study supervision: C. Dunham, S.E. Dunn

Acknowledgments

The authors thank Dr. Rob Wechsler-Reya for his scientific input.

Grant Support

This project was supported by the Michael Smith Foundation for Health Research, Hannah's Heroes Foundation, Summits of Hope, Mitacs, the Michael Cuccione Childhood Cancer Research Program, BrainCare BC, BC Children's Hospital Telethon, and the C17 Research Network.

The costs of publication of this article were defrayed in part by the payment of page charges. This article must therefore be hereby marked *advertisement* in accordance with 18 U.S.C. Section 1734 solely to indicate this fact.

Received November 23, 2012; revised April 10, 2013; accepted August 15, 2013; published OnlineFirst September 9, 2013.

References

- Agerlin N, Gjerris F, Brincker H, Haase J, Laursen H, Moller KA, et al. Childhood medulloblastoma in Denmark 1960–1984. A population-based retrospective study. *Childs Nerv Syst* 1999;15:29–36.
- Taillandier L, Blonski M, Carrie C, Bernier V, Bonnetain F, Bourdeaut F, et al. Medulloblastomas: review. *Rev Neurol* 2011;167:431–48.
- Sirachainan N, Nuchprayoon I, Thanarattanakorn P, Pakakasama S, Lusawat A, Visudibhan A, et al. Outcome of medulloblastoma in children treated with reduced-dose radiation therapy plus adjuvant chemotherapy. *J Clin Neurosci* 2011;18:515–9.
- Mabbott DJ, Spiegler BJ, Greenberg ML, Rutka JT, Hyder DJ, Bouffet E. Serial evaluation of academic and behavioral outcome after treatment with cranial radiation in childhood. *J Clin Oncol* 2005;23:2256–63.
- Northcott PA, Hielscher T, Dubuc A, Mack S, Shih D, Remke M, et al. Pediatric and adult sonic hedgehog medulloblastomas are clinically and molecularly distinct. *Acta Neuropathol* 2011;122:231–40.
- Ellison DW, Dalton J, Kocak M, Nicholson SL, Fraga C, Neale G, et al. Medulloblastoma: clinicopathological correlates of SHH, WNT, and non-SHH/WNT molecular subgroups. *Acta Neuropathol* 2011;121:381–96.
- Kool M, Korshunov A, Remke M, Jones DT, Schlanstein M, Northcott PA, et al. Molecular subgroups of medulloblastoma: an international meta-analysis of transcriptome, genetic aberrations, and clinical data of WNT, SHH, Group 3, and Group 4 medulloblastomas. *Acta Neuropathol* 2012;123:473–84.
- Northcott PA, Korshunov A, Witt H, Hielscher T, Eberhart CG, Mack S, et al. Medulloblastoma comprises four distinct molecular variants. *J Clin Oncol* 2011;29:1408–14.
- Lauth M, Bergstrom A, Shimokawa T, Toftgard R. Inhibition of GLI-mediated transcription and tumor cell growth by small-molecule antagonists. *Proc Natl Acad Sci U S A* 2007;104:8455–60.
- Yauch RL, Dijkgraaf GJ, Aliche B, Januario T, Ahn CP, Holcomb T, et al. Smoothed mutation confers resistance to a Hedgehog pathway inhibitor in medulloblastoma. *Science* 2009;326:572–4.
- Dijkgraaf GJ, Aliche B, Weinmann L, Januario T, West K, Modrusan Z, et al. Small molecule inhibition of GDC-0449 refractory smoothed mutants and downstream mechanisms of drug resistance. *Cancer Res* 2011;71:435–44.
- Buonamici S, Williams J, Morrissey M, Wang A, Guo R, Vattay A, et al. Interfering with resistance to smoothed antagonists by inhibition of the PI3K pathway in medulloblastoma. *Sci Transl Med* 2010;2:51ra70.
- Northcott PA, Shih DJ, Remke M, Cho YJ, Kool M, Hawkins C, et al. Rapid, reliable, and reproducible molecular sub-grouping of clinical medulloblastoma samples. *Acta Neuropathol* 2012;123:615–26.
- Tibshirani R, Hastie T, Narasimhan B, Chu G. Diagnosis of multiple cancer types by shrunken centroids of gene expression. *Proc Natl Acad Sci U S A* 2002;99:6567–72.
- Northcott PA, Korshunov A, Pfister SM, Taylor MD. The clinical implications of medulloblastoma subgroups. *Nat Rev Neurol* 2012;8:340–51.
- Fotovati A, Abu-Ali S, Wang PS, Deleyrolle LP, Lee C, Triscott J, et al. YB-1 bridges neural stem cells and brain-tumor initiating cells via its roles in differentiation and cell growth. *Cancer Res* 2011;71:5569–78.
- Lenkiewicz M, Li N, Singh SK. Culture and isolation of brain tumor initiating cells. *Curr Protoc Stem Cell Biol* 2009;Chapter 3:Unit 3
- Lee C, Fotovati A, Triscott J, Chen J, Venugopal C, Singhal A, et al. Polo-like kinase 1 inhibition kills glioblastoma multiforme brain tumor cells in part through loss of SOX2 and delays tumor progression in mice. *Stem Cells* 2012;30:1064–75.
- Hu K, Lee C, Qiu D, Fotovati A, Davies A, Abu-Ali S, et al. Small interfering RNA library screen of human kinases and phosphatases identifies polo-like kinase 1 as a promising new target for the treatment of pediatric rhabdomyosarcomas. *Mol Cancer Ther* 2009;8:3024–35.
- Stratford AL, Reipas K, Hu K, Fotovati A, Brough R, Frankum J, et al. Targeting p90 ribosomal S6 kinase eliminates tumor-initiating cells by inactivating Y-box binding protein-1 in triple-negative breast cancers. *Stem Cells* 2012;30:1338–48.
- Lee C, Dhillon J, Wang MY, Gao Y, Hu K, Park E, et al. Targeting YB-1 in HER-2 overexpressing breast cancer cells induces apoptosis via the mTOR/STAT3 pathway and suppresses tumor growth in mice. *Cancer Res* 2008;68:8661–6.
- Fouladi M, Gilger E, Kocak M, Wallace D, Buchanan G, Reeves C, et al. Intellectual and functional outcome of children 3 years old or younger who have CNS malignancies. *J Clin Oncol* 2005;23:7152–60.
- Yarm FR. Plk phosphorylation regulates the microtubule-stabilizing protein TCTP. *Mol Cell Biol* 2002;22:6209–21.
- Cucchi U, Gianellini LM, De Ponti A, Sola F, Alzani R, Patton V, et al. Phosphorylation of TCTP as a marker for polo-like kinase-1 activity in vivo. *Anticancer Res* 2010;30:4973–85.
- Shu Q, Antalffy B, Su JM, Adesina A, Ou CN, Pietsch T, et al. Valproic Acid prolongs survival time of severe combined immunodeficient mice bearing intracerebellar orthotopic medulloblastoma xenografts. *Clin Cancer Res* 2006;12:4687–94.
- Ahlfeld J, Favaro R, Pagella P, Kretzschmar HA, Nicolis S, Schuller U. Sox2 requirement in sonic hedgehog-associated medulloblastoma. *Cancer Res* 2013;73:3796–807.
- Elez R, Piiper A, Giannini CD, Brendel M, Zeuzem S. Polo-like kinase1, a new target for antisense tumor therapy. *Biochem Biophys Res Commun* 2000;269:352–6.
- Cogswell JP, Brown CE, Bisi JE, Neill SD. Dominant-negative polo-like kinase 1 induces mitotic catastrophe independent of cdc25C function. *Cell Growth Differ* 2000;11:615–23.
- Liu X, Lei M, Erikson RL. Normal cells, but not cancer cells, survive severe Plk1 depletion. *Mol Cell Biol* 2006;26:2093–108.
- Degenhardt Y, Lampkin T. Targeting polo-like kinase in cancer therapy. *Clin Cancer Res* 2010;16:384–9.
- Tokumitsu Y, Mori M, Tanaka S, Akazawa K, Nakano S, Niho Y. Prognostic significance of polo-like kinase expression in esophageal carcinoma. *Int J Oncol* 1999;15:687–92.
- Holtrich U, Wolf G, Brauningner A, Karn T, Bohme B, Rubsamen-Waigmann H, et al. Induction and down-regulation of PLK, a human serine/threonine kinase expressed in proliferating cells and tumors. *Proc Natl Acad Sci U S A* 1994;91:1736–40.
- Steegmaier M, Hoffmann M, Baum A, Lenart P, Petronczki M, Krssak M, et al. BI 2536, a potent and selective inhibitor of

- polo-like kinase 1, inhibits tumor growth in vivo. *Curr Biol* 2007; 17:316–22.
34. Frost A, Mross K, Steinbild S, Hedbom S, Unger C, Kaiser R, et al. Phase I study of the Plk1 inhibitor BI 2536 administered intravenously on three consecutive days in advanced solid tumours. *Curr Oncol* 2012;19:e28–35.
 35. Mross K, Frost A, Steinbild S, Hedbom S, Rentschler J, Kaiser R, et al. Phase I dose escalation and pharmacokinetic study of BI 2536, a novel Polo-like kinase 1 inhibitor, in patients with advanced solid tumors. *J Clin Oncol* 2008;26:5511–7.
 36. Rudolph D, Steegmaier M, Hoffmann M, Grauert M, Baum A, Quant J, et al. BI 6727, a Polo-like kinase inhibitor with improved pharmacokinetic profile and broad antitumor activity. *Clin Cancer Res* 2009;15:3094–102.
 37. Ma WW, Messersmith WA, Dy GK, Weekes CD, Whitworth A, Ren C, et al. Phase I study of Rigosertib, an inhibitor of the phosphatidylinositol 3-kinase and Polo-like kinase 1 pathways, combined with gemcitabine in patients with solid tumors and pancreatic cancer. *Clin Cancer Res* 2012;18:2048–55.
 38. Olmos D, Barker D, Sharma R, Brunetto AT, Yap TA, Taegtmeyer AB, et al. Phase I study of GSK461364, a specific and competitive Polo-like kinase 1 inhibitor, in patients with advanced solid malignancies. *Clin Cancer Res* 2011;17:3420–30.
 39. Medema RH, Lin CC, Yang JC. Polo-like kinase 1 inhibitors and their potential role in anticancer therapy, with a focus on NSCLC. *Clin Cancer Res* 2011;17:6459–66.
 40. Triscott J, Lee C, Hu K, Fotovati A, Berns R, Pambid M, et al. Disulfiram, a drug widely used to control alcoholism, suppresses the self-renewal of glioblastoma and over-rides resistance to temozolomide. *Oncotarget* 2012;3:1112–23.
 41. Harris PS, Venkataraman S, Alimova I, Birks DK, Donson AM, Knipstein J, et al. Polo-like kinase 1 (PLK1) inhibition suppresses cell growth and enhances radiation sensitivity in medulloblastoma cells. *BMC Cancer* 2012;12:80.
 42. Spaniol K, Boos J, Lanvers-Kaminsky C. An in-vitro evaluation of the polo-like kinase inhibitor GW843682X against paediatric malignancies. *Anticancer Drugs* 2011;22:531–42.
 43. Dhall G, Grodman H, Ji L, Sands S, Gardner S, Dunkel IJ, et al. Outcome of children less than three years old at diagnosis with non-metastatic medulloblastoma treated with chemotherapy on the "Head Start" I and II protocols. *Pediatr Blood Cancer* 2008; 50:1169–75.

Cancer Research

The Journal of Cancer Research (1916–1930) | The American Journal of Cancer (1931–1940)

Personalizing the Treatment of Pediatric Medulloblastoma: Polo-like Kinase 1 as a Molecular Target in High-Risk Children

Joanna Triscott, Cathy Lee, Colleen Foster, et al.

Cancer Res 2013;73:6734-6744. Published OnlineFirst September 9, 2013.

Updated version	Access the most recent version of this article at: doi: 10.1158/0008-5472.CAN-12-4331
Supplementary Material	Access the most recent supplemental material at: http://cancerres.aacrjournals.org/content/suppl/2013/09/12/0008-5472.CAN-12-4331.DC1

Cited articles	This article cites 42 articles, 24 of which you can access for free at: http://cancerres.aacrjournals.org/content/73/22/6734.full.html#ref-list-1
-----------------------	--

Citing articles	This article has been cited by 7 HighWire-hosted articles. Access the articles at: /content/73/22/6734.full.html#related-urls
------------------------	---

E-mail alerts	Sign up to receive free email-alerts related to this article or journal.
----------------------	--

Reprints and Subscriptions	To order reprints of this article or to subscribe to the journal, contact the AACR Publications Department at pubs@aacr.org .
-----------------------------------	--

Permissions	To request permission to re-use all or part of this article, contact the AACR Publications Department at permissions@aacr.org .
--------------------	---